Variational Ansatz for an Abelian to Non-Abelian Topological Phase Transition in $\nu = 1/2 + 1/2$ Bilayers

Valentin Crépel,[1] Benoit Estienne,[2] and Nicolas Regnault[1]
[1]*Laboratoire de Physique de l'École normale supérieure, ENS, Université PSL, CNRS, Sorbonne Université, Université Paris-Diderot, Sorbonne Paris Cité, 75005 Paris, France*
[2]*Sorbonne Université, CNRS, Laboratoire de Physique Théorique et Hautes Énergies, LPTHE, F-75005 Paris, France*

(Received 9 April 2019; published 20 September 2019)

We propose a one-parameter variational ansatz to describe the tunneling-driven Abelian to non-Abelian transition in bosonic $\nu = 1/2 + 1/2$ fractional quantum Hall bilayers. This ansatz, based on exact matrix product states, captures the low-energy physics all along the transition and allows us to probe its characteristic features. The transition is continuous, characterized by the decoupling of antisymmetric degrees of freedom. We futhermore determine the tunneling strength above which non-Abelian statistics should be observed experimentally. Finally, we propose to engineer the interlayer tunneling to create an interface trapping a neutral chiral Majorana fermion. We microscopically characterize such an interface using a slightly modified model wave function.

DOI: 10.1103/PhysRevLett.123.126804

Introduction.—Fractional quantum Hall (FQH) systems are to date the most promising platform to investigate phases of matter with intrinsic topological order [1–4]. Innovative experimental advances on heterostructural design [5–8] rapidly promoted these new setups as highly competitive for the study of strongly correlated quantum phases [9,10]. At the same time, new layer-sensitive spectroscopic techniques are developed in wide and double quantum wells [11,12], which allowed us to probe the long discussed condensation of excitons [13]. The inner (valley or layer) degree of freedom (d.o.f.) in these systems offers additional tunable parameters [14,15] and enriches the phase diagram [16–18]. This revives the interest in engineering non-Abelian topological phases from coupling internal d.o.f. of multicomponent FQH systems [19–23], which are initially prepared in a well controlled Abelian state [24,25].

Theoretically, the simplest construction of such an Abelian to non-Abelian transition starts with an Halperin 220 state [26] at a total filling fraction $\nu = 1$. It describes two decoupled copies of the bosonic Laughlin $1/2$ wave function (WF) [2,24]. Symmetrization of the two copies [27–30] leads to the non-Abelian bosonic Pfaffian state [31]. Symmetry gauging arguments [32–34] have shown that this procedure not only relates the two WFs, but it also produces the full non-Abelian Pfaffian topological order [4] from the Abelian Halperin one [35]. It was argued [21] that interlayer tunneling could physically drive such a symmetrization of the low energy d.o.f. This statement was put on firmer ground by considering the effect of tunneling on the one-dimensional effective theory at the edge of the system [36,37], while numerical studies have repeatedly confirmed that the tunneling-driven Abelian to non-Abelian transition occurs at a microscopic level in bilayer FQH systems [15,38–44].

Model WFs have widely contributed to our understanding of correlated phases of quantum matter such as the BCS ansatz [45–47] and FQH model states [2,24–26,31]. Their physical relevance were soon corroborated by the finding of Hamiltonians for which they are the exact ground state: the Bogoliubov approach to superconductivity [48,49] and model N-body interactions for the FQHE [50–52]. Although the interactions stabilizing the FQH model states are not realistic [53], the corresponding ground state WFs nonetheless capture the universal features of the phase such as quasiparticle charge and braiding statistics in the bulk and quasihole exponents on the gapless edge. The connection between FQH phases and the underlying topological order was considerably substantiated by Moore and Read in Ref. [31]. They identified a large class of model WFs and their quasihole excitations with conformal field theory (CFT) correlators from which the topological content of the phase may be read off (under the generalized screening assumption [54]). It furthermore allows for an exact matrix product state (MPS) description of these strongly correlated phases of matter [55–57], allowing for large scale numerical study of their relevance and properties [58,59].

In this Letter, we propose a variational ansatz based on the CFT description in order to fully capture the low energy physics of a bosonic FQH bilayer with *arbitrary* interlayer tunneling. The MPS description allows us to observe a continuous phase transition driven by the decoupling of antisymmetric d.o.f. We also determine the precise range of tunneling where a non-Abelian order fully develops.

Microscopic model.—We study a two-component bosonic system at total filling $\nu = 1$ in the FQH regime.

Bosons populate the lowest band assumed to be a Chern band with $\mathcal{C}=1$ [60], nearly flat and separated from the other ones by a large gap. For simplicity, we focus on the continuum limit where a large uniform magnetic field (possibly artificial [61,62]) produces exactly flat Landau levels. Temperature and interaction strength are supposed to be small enough to avoid a Landau level mixing, allowing projection onto the lowest Landau level (LLL). The layer d.o.f. forms a pseudo spin-1/2 with z components $\sigma \in \{\uparrow,\downarrow\}$. Although we will use the vocabulary of bilayer systems, our discussion extends to any other type of two-dimensional internal d.o.f. such as spin, hyperfine states of an atom, and so on. As kinetic energy is frozen, the interactions projected to the LLL dominate and produce strong correlations between particles. We assume density-density interactions within each layer to be

$$\mathcal{H}_{\mathrm{int}} = J \int d^2z \sum_{\sigma\in\{\uparrow,\downarrow\}} :\rho_\sigma(z)\rho_\sigma(z):, \tag{1}$$

where we have defined $\rho_\sigma(z)$ as the LLL projected density in layer σ at position z. The interaction strength J is set such that the two-body problem only has eigenvalues zero and one on the infinite cylinder. The densest ground state of Eq. (1) is the Halperin 220 state [50,63]. It has a fourfold topological degeneracy on the torus, corresponding to the four anyons of the underlying Abelian topological order [35]. Under the global layer permutation $\mathcal{P}_z$ (swapping $\uparrow$ and $\downarrow$), which commutes with $\mathcal{H}_{\mathrm{int}}$, three of them are even while the last one is odd [64]. Coupling of the two layers is achieved by introducing tunneling as $\mathcal{H}_{\mathrm{tun}} = -tS_x$. It acts as a Zeeman term coupling to the x components of the total spin $\mathbf{S}$ and splits the Halperin 220 ground state manifold into even and odd sectors. With increasing tunneling strengths, the odd-parity state crosses the gap and ultimately merges into the many-body spectrum continuum [38]. The remaining threefold ground state degeneracy is a signal of the non-Abelian Pfaffian topological order [31], which we can understand as follows. Tunneling splits the LLL into two subbands, gathering, respectively, single-particle WFs with layer index in the two pseudospin x eigenstates, which we denote as even $e=(\uparrow+\downarrow)/\sqrt{2}$ and odd $o=(\uparrow-\downarrow)/\sqrt{2}$. At a large tunneling $t\gg 1$, the system behaves as an effective single-component FQH system fully polarized in e, due to the large subband Zeeman gap, with delta interactions. We rely on numerical studies to certify that its ground state is well approximated by the non-Abelian Pfaffian state [40,64].

Model state.—Motivated by the solution of a specific model of spin-triplet pairing in p-wave superconductors displaying a similar tunneling-driven Abelian to non-Abelian transition [21,30,65–68], we propose the following one-parameter ansatz for the low energy theory of $\mathcal{H}_{\mathrm{int}}+\mathcal{H}_{\mathrm{tun}}$:

$$|\Psi_\theta\rangle\!\rangle = \langle 0|\mathcal{O}_{\mathrm{Bkg}} \exp\Big(\int d^2z[\cos\theta \mathcal{V}^e(z)\otimes c_e^\dagger(z) + \sin\theta \mathcal{V}^o(z)\otimes c_o^\dagger(z)]\Big)|0\rangle \otimes |\Omega\rangle\!\rangle, \quad \theta\in[0,\pi/4]. \tag{2}$$

Here, $c_{e/o}^\dagger(z)$ creates a boson in the spin component e/o at position z above the Fock vacuum $|\Omega\rangle\!\rangle$. $|0\rangle$ is the CFT vacuum state. The CFT uses two chiral bosonic field ϕ^s and ϕ^c [69] to encode the spin and charge the d.o.f. that decouple on the edge of the system [70,71]. ϕ^c carries a U(1) charge associated with particle number. The neutralizing background charge $\mathcal{O}_{\mathrm{Bkg}}$ fixes the overall number of particles and reproduces the Gaussian factors of the LLL [31,72]. Spin excitations are described by a Dirac fermion $\Psi^\dagger =: e^{i\phi^s}:$ [29,36]. Its real and imaginary parts are related to the spin in the x direction. The operators associated with the bosonic creation operators in Eq. (2) are

$$\mathcal{V}^e =: \cos(\phi^s)e^{i\phi^c}:, \qquad \mathcal{V}^o = i:\sin(\phi^s)e^{i\phi^c}:. \tag{3}$$

Our ansatz smoothly interpolates between the Pfaffian and the Halperin 220 state, which are exactly reproduced, respectively, for $\theta=0$ and $\theta=\pi/4$ [30]. As θ goes to zero, the total spin of the variational ansatz polarizes in the e component, which drives the transition discussed above.

Being written as a CFT correlator, our ansatz can be brought to an MPS form. All numerical calculations are performed on a cylinder of perimeter L (measured in units of magnetic length ℓ_B), the efficient geometry for the FQH MPS formulation [56,73,74]. We first computed the overlap between the ED ground state of lowest momentum for several tunneling strength t. The best variational parameter $\theta_{\mathrm{ED}}^{\max}(t)$ is depicted in Fig. 1. Since both the Halperin 220 and the Pfaffian states belong to the optimization set, it is not surprising that our ansatz performs better than these two model states (also displayed in Fig. 1). However in the transition region where they both fail to capture the low energy physics, our ansatz remains a very good approximation of the ground state. Hence, the theoretical ingredients used to build Eq. (2) seem to faithfully account for the low energy physics of the model for any tunneling. To confirm that these high overlaps are not merely the artifacts of the optimization procedure, we can fix the variational parameter *independently* by minimizing the energy per orbital on an infinite cylinder. We developed a method to evaluate the interaction $E(\theta)=\langle\!\langle\Psi_\theta|\mathcal{H}_{\mathrm{int}}|\Psi_\theta\rangle\!\rangle$ and tunneling $T(\theta)=\langle\!\langle\Psi_\theta|\mathcal{H}_{\mathrm{tun}}|\Psi_\theta\rangle\!\rangle$ energies that bypasses the use of matrix product operators [30]. In essence, we have adapted known results about continuous MPS [75] to our ansatz $|\Psi_\theta\rangle\!\rangle$, seeing it as a Hamiltonian time evolution of a 1D CFT [72]. The energy minimization procedure fixes the variational parameter $\theta_{\mathrm{iMPS}}^{\max}(t)$, as depicted in Fig. 1. We find an excellent agreement between the numerically

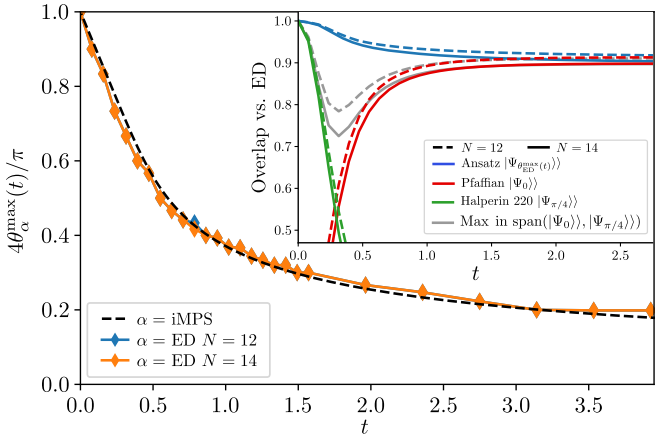

FIG. 1. Comparison of our ansatz with the lowest momentum ED ground state on a cylinder of perimeter $L = 8\ell_B$. Main: The variational parameter $\theta_{\text{ED}}^{\max}(t)$ maximizing the overlap for $N = 12$ and $N = 14$ particles as a function of tunneling (diamonds). It agrees extremely well with $\theta_{\text{iMPS}}^{\max}(t)$ determined independently by energy minimization on an infinite cylinder (dashed line). Inset: Best overlap with our variational ansatz (blue) for two system sizes as a function of the tunneling strength t. For comparison, the overlap with the Pfaffian (red) and Halperin 220 (green) states are also provided together with the best overlap in the vector space that they generate (gray).

extracted $\theta_{\text{iMPS}}^{\max}(t)$ and our previous finite size results $\theta_{\text{ED}}^{\max}(t)$. This provides another stringent test of the physical relevance of our ansatz.

Continuous transition.—To be immune to local perturbations and exhibit topological order, a system should be gapped (or screened in the FQH language); i.e., correlation function of local observables must decay exponentially with distance. In the MPS formalism, a local excitation such as $c_e(z)|\Psi_\theta\rangle\rangle$ is translated into the insertion of $\mathcal{V}^e$ [see Eq. (2)] which couples to an excited state of the transfer matrix. The correlation length governing the decay of $\langle\langle\Psi_\theta|c_e^\dagger(z)c_e(w)|\Psi_\theta\rangle\rangle$ is then related to the corresponding eigenvalue of the transfer matrix [58,76]. While bulk excitations generically couple to the first excited state of the transfer matrix, the $\mathcal{P}_z$ symmetry, which translates into $\phi^s \to -\phi^s$ in the CFT, imposes further selection rules. Symmetric (respectfully, antisymmetric) excitations under layer inversion couple to even (respectfully, odd) excited state under $\mathcal{P}_z$. We extracted the corresponding even ξ_{loc}^e and odd ξ_{loc}^o correlation lengths as a function of θ, as shown in Fig. 2. The correlation length ξ_{loc}^e is finite for all θ and smoothly interpolates between the values of Refs. [58,77] for the Halperin 220 and the one-component bosonic Pfaffian states. We observe that antisymmetric excitations are not equally well screened and that ξ_{loc}^o diverges when θ goes to zero. We relate these features to the depletion of the o band. Notice indeed that $\mathcal{V}^o$ insertions in Eq. (2) are only screened by o electrons with which they have nontrivial fusion rules. Linear response theory predicts that ξ_{loc}^o is inversely proportional to ν_o when the filling factor of the o band goes to zero. We find that this law accurately accounts for the computed ξ_{loc}^o, as depicted in Fig. 2. We shall now argue that this critical behavior at small θ remains unnoticed. Take $\theta = 0$, the system has no o particles [see Eq. (2)] and only couples to the symmetric part of local observables, for instance:

$$\langle\langle\Psi_0|c_\uparrow^\dagger(z)c_\uparrow(w)|\Psi_0\rangle\rangle = \langle\langle\Psi_0|c_e^\dagger(z)c_e(w)|\Psi_0\rangle\rangle. \quad (4)$$

This creates some redundancies in the MPS description since the antisymmetric part of the ϕ^s field is conserved. The corresponding d.o.f. on the MPS boundary condition lead to exact degeneracies in the transfer matrix spectrum and explain the divergence of ξ_{loc}^o at $\theta = 0$. Note however that all these different MPS boundary conditions are completely transparent to the e particles and produce the *same* physical state. For $\theta \lesssim \pi/20$, the bands are only weakly coupled, as shown in Fig. 2. The system is almost polarized $\nu_o \ll \nu_e$ and exhibit a clear scale separation $\xi_{\text{loc}}^e \ll \xi_{\text{loc}}^o$. The previous degeneracies are slightly lifted and excitations in the empty o band form a gapless branch above the ground state. However, o d.o.f. only become noticeable at very large scales $\sim\xi_{\text{loc}}^o$. For instance, the first correction to Eq. (4) is of order $\sqrt{\nu_o}e^{-|z-w|/\xi_{\text{loc}}^o}$, small in magnitude unless the even excitation is fully screened. Low ν_o population makes these excitations transparent on the scale over which the correlation builds up in the e band, such that the ground state properties are locally that of the

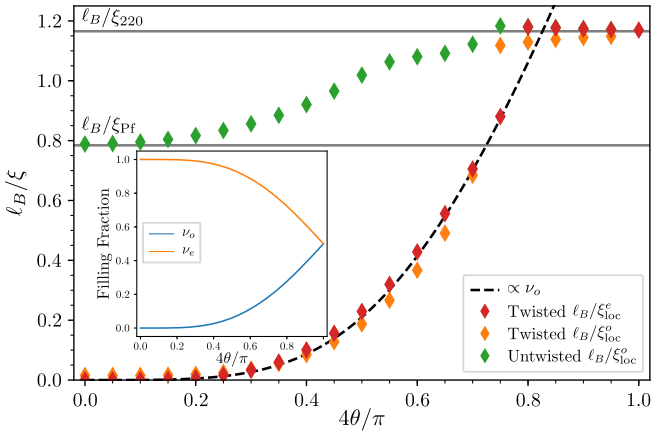

FIG. 2. Main: Inverse of the even and odd correlation lengths as a function of the variational parameter. The even correlation length ξ_{loc}^e remains finite and interpolates between the Halperin 220 ξ_{220} and Pfaffian ξ_{Pf} values. The odd correlation length, computed in the twisted and untwisted sectors (see below), diverges as $\ell_B/\xi_{\text{loc}}^o \propto \nu_o$ when $\theta \to 0$ (see text). For $4\theta/\pi > 0.7$, a level crossing in the spectrum prevents us to follow the corresponding transfer matrix eigenstate. Inset: Filling fraction ν_o in blue (respectfully, ν_e in orange) of the odd (respectfully, even) LLL band of Eq. (2).

$\theta = 0$ point. Similar behaviors are observed for anyon-anyon correlation functions [30,78,79].

Non-Abelian properties.—At $\theta = 0$, we saw that the odd excitations decouple from the low-energy d.o.f. of the system. Splitting the Halperin 220 anyonic excitations into even and odd parts under $\mathcal{P}_z$, we are left with two deconfined anyons ψ and $\sigma =: \cos(\phi^s/2)e^{(i/2)\phi^c}:$ obeying the fusion rules:

$$\psi \times \psi = \mathbf{1}, \qquad \psi \times \sigma = \sigma, \qquad \sigma \times \sigma = \mathbf{1} + \psi. \quad (5)$$

They define an $SU(2)_2$ algebra [80], which characterizes the Pfaffian topological order [31]. The previous discussion about the correlation lengths establishes that the same non-Abelian theory extends above this special point, here for $\theta \lesssim \pi/20$. The Pfaffian physics can be probed by braiding anyons kept by a few ξ^e_{loc} apart and the observed separation of scale ensures that odd contributions do not spoil the results. Going from the Halperin 220 order to Eq. (5) can be interpreted as gauging the symmetry $\mathcal{P}_z$ [33,81], which is indeed locally satisfied when the system is fully polarized in e, followed by the deconfinement of the symmetry defects [34], which we couldn't probe directly though we believe it to be related to the ξ^o_{loc} divergence. Restoring the Abelian order from Eq. (5) can be viewed as a condensing of the boson $i\partial\phi^s$ [32].

To test the non-Abelian character at small θ and put bound on the Pfaffian regime in the phase diagram, we evaluated the constant correction to the entanglement area law, the topological entanglement entropy (TEE) [82,83], which is known to characterize the topological order. We rely on the ansatz structure [30] to computed the real-space entanglement entropy $S(\theta)$ of Eq. (2) in all sectors, for a cut preserving the cylinder rotational symmetry [84–86]. The TEE is then extracted by finite difference with respect to the cylinder perimeter, as in Refs. [57,87,88]. The numerical results for one twisted and one untwisted sector are depicted in Fig. 3. Identical results were found for both members of the (un)twisted pair, which are related by a center of mass translation corresponding to a shift of the U(1) charge at the MPS boundary. When $\theta \simeq \pi/4$, all four sectors have the same TEE $\gamma \simeq 2\log\sqrt{2}$ matching the prediction for the Abelian Halperin 220 topological order [35,89]. For $\theta \lesssim \pi/20$, we find $\gamma_{\mathbb{I}} = \gamma_{\psi} \simeq \log\sqrt{4}$ in the untwisted sectors, and $\gamma_{\sigma} \simeq \log\sqrt{2}$ in the twisted sector. The different sectors having distinct TEE is an indication of the non-Abelian nature of the phase. The extracted TEEs agree with the quantum dimensions of the $\mathbb{I}$, ψ, and σ anyons [80]. These results bolster the physical picture depicted above. They also provide a quantitative range θ and hence in t over which the system exhibit a true Abelian ($\theta \in [\pi/5, \pi/4]$, $t \in [0, 0.2162(1)]$) or non-Abelian ($\theta \in [0, \pi/20]$, $t \in [2.74(7), \infty]$) order.

Trapping a Majorana fermion.—It is argued that a one-dimensional neutral chiral Majorana fermion is trapped at the interface between a Halperin 220 phase and a Pfaffian phase [37,80]. Our study provides a simple protocol to realize such a setup microscopically, varying the tunneling parameter spatially. Let $t(x)$ vary smoothly along the cylinder axis such that the Halperin 220 and Pfaffian phases are stabilized on either sides of the interface, where the interaction Eq. (1) mixes their counterpropagating edge modes. Assuming that all interface d.o.f. present on both sides gap out [37,80], only the antisymmetric edge excitations remain. They are described by a chiral Majorana fermion ψ^I, the imaginary part of Ψ.

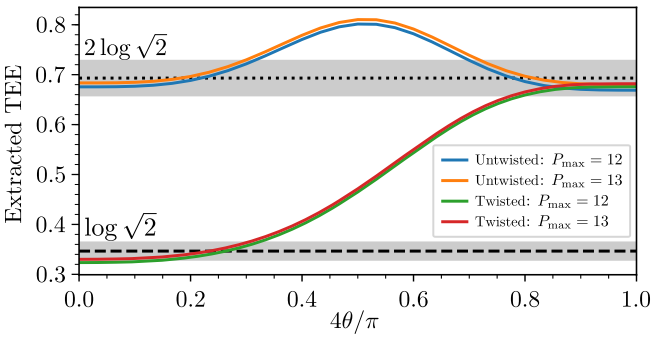

FIG. 3. Extraction of the TEE at $L = 10\ell_B$ in the twisted and untwisted sectors using the method of Ref. [77]. Dotted lines indicate theoretical predictions and gray shaded areas around them represent a 5% deviation. While we are still off these predictions by a few percents in the Halperin 220 and Pfaffian phases, increasing the MPS bond dimension measured by $P_{\max}$ [30] brings our results closer to the expected values.

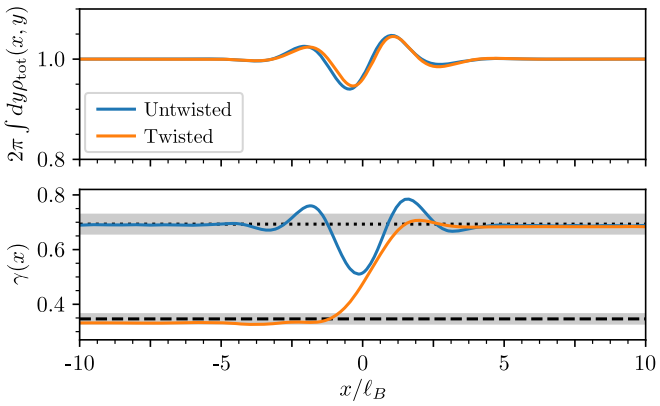

FIG. 4. Top: Total density integrated over the cylinder perimeter across the interface. It is featureless, but for small ripples that are certainly due to the sharpness of our interface ansatz (see Refs. [87,88]). We checked that no charge accumulates at the interface, even for excitations of ψ^I, showing that the interface effective theory is neutral. Bottom: Extracted TEE in the twisted and untwisted sectors at different position across the interface. We recover the values characterizing the Pfaffian and Halperin 220 phases away from the interface $|x| \gg \ell_B$, showing the relevance of the interface MPS WF.

We can numerically probe such an interface between distinct topological orders within the MPS formalism as first described in Refs. [87,88]. A model WF describing a sharp interface at $x = 0$ is built by using the Halperin (respectfully, Pfaffian) MPS matrices for LLL orbitals centered at $x > 0$ (respectfully, $x < 0$). This interface model WF was shown to capture all universal as well as some microscopic features of the interface [87,88]. We first extract the TEE $\gamma(x)$ at a different position x, the results are depicted in Fig. 4(bottom). Deep in the two phases, we retrieve the expected TEE for the Halperin 220 and Pfaffian phases, which proves that our interface model WF indeed interpolates between the two topological orders. Next, we observe that, besides small ripples, the density is completely featureless across the interface [see Fig. 4(top)]. We checked this to also be true for excited state of ψ^I, which shows that the interface edge mode is neutral. To further characterize the interface low-energy effective theory, we extracted its chiral anomaly (or central charge) c following the methods developed in Refs. [87,88]. We find that $c \simeq 1/2$ [30], for which the only unitary minimal model is that of a free Majorana fermion [69,90].

Conclusion.—In this Letter, we extended the CFT approach to bulk FQH WFs to describe a continuous phase transition between distinct topological orders. Besides the two fixed points on either sides of the transition, it accurately describes the low-energy physics of FQH bosonic bilayers at arbitrary tunneling. We used it to observe the characteristic features of the Abelian to non-Abelian transition and could put bounds on each domains. Finally, we showed that a neutral Majorana fermion could be trapped at an interface engineered by spatially varying the tunneling strength.

We thank Y. Fuji, J. Slingerland, and P. Lecheminant for enlightening discussions. V. C., B. E., and N. R. were supported by the Grants ANR TNSTRONG No. ANR-16-CE30-0025 and ANR TopO No. ANR-17-CE30-0013-01.

[1] D. C. Tsui, H. L. Stormer, and A. C. Gossard, Two-Dimensional Magnetotransport in the Extreme Quantum Limit, Phys. Rev. Lett. **48**, 1559 (1982).
[2] R. B. Laughlin, Anomalous Quantum Hall Effect: An Incompressible Quantum Fluid with Fractionally Charged Excitations, Phys. Rev. Lett. **50**, 1395 (1983).
[3] X.-G. Wen, Topological orders in rigid states, Int. J. Mod. Phys. B **04**, 239 (1990).
[4] C. Nayak and F. Wilczek, 2n-quasihole states realize 2n-1-dimensional spinor braiding statistics in paired quantum hall states, Nucl. Phys. **B479**, 529 (1996).
[5] B. Hunt, J. D. Sanchez-Yamagishi, A. F. Young, M. Yankowitz, B. J. LeRoy, K. Watanabe, T. Taniguchi, P. Moon, M. Koshino, P. Jarillo-Herrero, and R. C. Ashoori, Massive dirac fermions and hofstadter butterfly in a van der waals heterostructure, Science **340**, 1427 (2013).
[6] A. A. Zibrov, C. Kometter, H. Zhou, E. M. Spanton, T. Taniguchi, K. Watanabe, M. P. Zaletel, and A. F. Young, Tunable interacting composite fermion phases in a half-filled bilayer-graphene landau level, Nature (London) **549**, 360 (2017).
[7] E. M. Spanton, A. A. Zibrov, H. Zhou, T. Taniguchi, K. Watanabe, M. P. Zaletel, and A. F. Young, Observation of fractional chern insulators in a van der waals heterostructure, Science **360**, 62 (2018).
[8] C. Jin, E. C. Regan, A. Yan, M. Iqbal Bakti Utama, D. Wang, S. Zhao, Y. Qin, S. Yang, Z. Zheng, S. Shi, K. Watanabe, T. Taniguchi, S. Tongay, A. Zettl, and F. Wang, Observation of moiré excitons in wse2/ws2 heterostructure superlattices, Nature (London) **567**, 76 (2019).
[9] Y. Cao, V. Fatemi, A. Demir, S. Fang, S. L. Tomarken, J. Y. Luo, J. D. Sanchez-Yamagishi, K. Watanabe, T. Taniguchi, E. Kaxiras, R. C. Ashoori, and P. Jarillo-Herrero, Correlated insulator behaviour at half-filling in magic-angle graphene superlattices, Nature (London) **556**, 80 (2018).
[10] Y. Cao, V. Fatemi, S. Fang, K. Watanabe, T. Taniguchi, E. Kaxiras, and P. Jarillo-Herrero, Unconventional superconductivity in magic-angle graphene superlattices, Nature (London) **556**, 43 (2018).
[11] A. Kogar, M. S. Rak, S. Vig, A. A. Husain, F. Flicker, Y. Il Joe, L. Venema, G. J. MacDougall, T. C. Chiang, E. Fradkin, J. van Wezel, and P. Abbamonte, Signatures of exciton condensation in a transition metal dichalcogenide, Science **358**, 1314 (2017).
[12] J. P. Eisenstein, L. N. Pfeiffer, and K. W. West, Interlayer interactions and the fermi energy of bilayer composite-fermion metals, Phys. Rev. B **98**, 201406(R) (2018).
[13] J. P. Eisenstein and A. H. MacDonald, Bose-einstein condensation of excitons in bilayer electron systems, Nature (London) **432**, 691 (2004).
[14] B. I. Halperin, Theories for $\nu = \{1\}/\{2\}$ in single- and double-layer systems, Surf. Sci. **305**, 1 (1994).
[15] Z. Papić, M. O. Goerbig, N. Regnault, and M. V. Milovanović, Tunneling-driven breakdown of the 331 state and the emergent pfaffian and composite fermi liquid phases, Phys. Rev. B **82**, 075302 (2010).
[16] J. Jung, A. Raoux, Z. Qiao, and A. H. MacDonald, *Ab initio* theory of moiré superlattice bands in layered two-dimensional materials, Phys. Rev. B **89**, 205414 (2014).
[17] M. Xie and A. H. MacDonald, On the nature of the correlated insulator states in twisted bilayer graphene, arXiv:1812.04213.
[18] K. L. Seyler, P. Rivera, H. Yu, N. P. Wilson, E. L. Ray, D. G. Mandrus, J. Yan, W. Yao, and X. Xu, Signatures of moiré-trapped valley excitons in mose2/wse2 heterobilayers, Nature (London) **567**, 66 (2019).
[19] B. I. Halperin, Statistics of Quasiparticles and the Hierarchy of Fractional Quantized Hall States, Phys. Rev. Lett. **52**, 1583 (1984).
[20] F. D. M. Haldane and E. H. Rezayi, Spin-Singlet Wave Function for the Half-Integral Quantum Hall Effect, Phys. Rev. Lett. **60**, 956 (1988).
[21] N. Read and Dmitry Green, Paired states of fermions in two dimensions with breaking of parity and time-reversal symmetries and the fractional quantum hall effect, Phys. Rev. B **61**, 10267 (2000).

[22] E. Fradkin, C. Nayak, A. Tsvelik, and F. Wilczek, A chern-simons effective field theory for the pfaffian quantum hall state, Nucl. Phys. **B516**, 704 (1998).

[23] E. Fradkin, C. Nayak, and K. Schoutens, Landau-ginzburg theories for non-Abelian quantum hall states, Nucl. Phys. **B546**, 711 (1999).

[24] R. B. Laughlin, Elementary theory: The incompressible quantum fluid, in *The Quantum Hall Effect*, edited by Richard E. Prange and Steven M. Girvin (Springer, New York, 1990), pp. 233–301.

[25] J. K. Jain, Composite-Fermion Approach for the Fractional Quantum Hall Effect, Phys. Rev. Lett. **63**, 199 (1989).

[26] B. Halperin, Theory of the quantized hall conductance, Helv. Acta Phys. **56**, 75 (1983).

[27] C. Repellin, T. Neupert, B. A. Bernevig, and N. Regnault, Projective construction of the z_k read-rezayi fractional quantum hall states and their excitations on the torus geometry, Phys. Rev. B **92**, 115128 (2015).

[28] A. Cappelli, L. S. Georgiev, and I. T. Todorov, Parafermion hall states from coset projections of Abelian conformal theories, Nucl. Phys. **B599**, 499 (2001).

[29] D. C. Cabra, A. Lopez, and G. L. Rossini, Transition from Abelian to non-Abelian FQHE states, Eur. Phys. J. B **19**, 21 (2001).

[30] See Supplemental Material at http://link.aps.org/supplemental/10.1103/PhysRevLett.123.126804 for additional details on the model wave functions and the numerical computations.

[31] G. Moore and N. Read, Nonabelions in the fractional quantum hall effect, Nucl. Phys. **B360**, 362 (1991).

[32] M. Barkeshli and X.-G. Wen, Bilayer quantum hall phase transitions and the orbifold non-Abelian fractional quantum hall states, Phys. Rev. B **84**, 115121 (2011).

[33] M. Barkeshli, P. Bonderson, M. Cheng, and Z. Wang, Symmetry, defects, and gauging of topological phases, arXiv:1410.4540.

[34] J. C. Y. Teo, T. L. Hughes, and E. Fradkin, Theory of twist liquids: Gauging an anyonic symmetry, Ann. Phys. (Amsterdam) **360**, 349 (2015).

[35] X. G. Wen and A. Zee, Classification of Abelian quantum hall states and matrix formulation of topological fluids, Phys. Rev. B **46**, 2290 (1992).

[36] J. D. Naud, L. P. Pryadko, and S. L. Sondhi, Quantum hall bilayers and the chiral sine-gordon equation, Nucl. Phys. **B565**, 572 (2000).

[37] K. Yang, Interface and phase transition between moore-read and halperin 331 fractional quantum hall states: Realization of chiral majorana fermion, Phys. Rev. B **96**, 241305(R) (2017).

[38] W. Zhu, S. S. Gong, D. N. Sheng, and L. Sheng, Possible non-Abelian moore-read state in double-layer bosonic fractional quantum hall system, Phys. Rev. B **91**, 245126 (2015).

[39] W. Zhu, Z. Liu, F. D. M. Haldane, and D. N. Sheng, Fractional quantum hall bilayers at half filling: Tunneling-driven non-Abelian phase, Phys. Rev. B **94**, 245147 (2016).

[40] N. Regnault, M. O. Goerbig, and Th. Jolicoeur, Bridge between Abelian and Non-Abelian Fractional Quantum Hall States, Phys. Rev. Lett. **101**, 066803 (2008).

[41] S. Geraedts, M. P. Zaletel, Z. Papić, and R. S. K. Mong, Competing Abelian and non-Abelian topological orders in $\nu = 1/3 + 1/3$ quantum hall bilayers, Phys. Rev. B **91**, 205139 (2015).

[42] N. Regnault and Th. Jolicoeur, Quantum hall fractions for spinless bosons, Phys. Rev. B **69**, 235309 (2004).

[43] S. Furukawa and M. Ueda, Quantum hall phase diagram of two-component bose gases: Intercomponent entanglement and pseudopotentials, Phys. Rev. A **96**, 053626 (2017).

[44] S. D. Geraedts, C. Repellin, C. Wang, R. S. K. Mong, T. Senthil, and N. Regnault, Emergent particle-hole symmetry in spinful bosonic quantum hall systems, Phys. Rev. B **96**, 075148 (2017).

[45] L. N. Cooper, Bound electron pairs in a degenerate fermi gas, Phys. Rev. **104**, 1189 (1956).

[46] J. Bardeen, L. N. Cooper, and J. R. Schrieffer, Microscopic theory of superconductivity, Phys. Rev. **106**, 162 (1957).

[47] J. Bardeen, L. N. Cooper, and J. R. Schrieffer, Theory of superconductivity, Phys. Rev. **108**, 1175 (1957).

[48] N. N. Bogoliubov, A new method in the theory of superconductivity i, Sov. Phys. JETP-USSR **7**, 794 (1958).

[49] N. N. Bogoljubov, V. V. Tolmachov, and D. V. Sirkov, A new method in the theory of superconductivity, Fortschr. Phys. **6**, 605 (1958).

[50] S. A. Trugman and S. Kivelson, Exact results for the fractional quantum hall effect with general interactions, Phys. Rev. B **31**, 5280 (1985).

[51] F. D. M. Haldane, Fractional Quantization of the Hall Effect: A Hierarchy of Incompressible Quantum Fluid States, Phys. Rev. Lett. **51**, 605 (1983).

[52] B. A. Bernevig and F. D. M. Haldane, Generalized clustering conditions of jack polynomials at negative jack parameter α, Phys. Rev. B **77**, 184502 (2008).

[53] F. D. M. Haldane, The hierarchy of fractional states and numerical studies, in *The Quantum Hall Effect*, edited by R. E. Prange and S. M. Girvin (Springer, New York, 1990), pp. 303–352.

[54] P. Bonderson, V. Gurarie, and C. Nayak, Plasma analogy and non-Abelian statistics for ising-type quantum hall states, Phys. Rev. B **83**, 075303 (2011).

[55] J. Ignacio Cirac and G. Sierra, Infinite matrix product states, conformal field theory, and the haldane-shastry model, Phys. Rev. B **81**, 104431 (2010).

[56] M. P. Zaletel and R. S. K. Mong, Exact matrix product states for quantum hall wave functions, Phys. Rev. B **86**, 245305 (2012).

[57] B. Estienne, N. Regnault, and B. A. Bernevig, Fractional quantum Hall matrix product states for interacting conformal field theories, arXiv:1311.2936.

[58] B. Estienne, N. Regnault, and B. A. Bernevig, Correlation Lengths and Topological Entanglement Entropies of Unitary and Nonunitary Fractional Quantum Hall Wave Functions, Phys. Rev. Lett. **114**, 186801 (2015).

[59] Y.-L. Wu, B. Estienne, N. Regnault, and B. A. Bernevig, Braiding Non-Abelian Quasiholes in Fractional Quantum Hall States, Phys. Rev. Lett. **113**, 116801 (2014).

[60] D. J. Thouless, M. Kohmoto, M. P. Nightingale, and M. den Nijs, Quantized Hall Conductance in a Two-Dimensional Periodic Potential, Phys. Rev. Lett. **49**, 405 (1982).

[61] J. Dalibard, Introduction to the physics of artificial gauge fields, arXiv:1504.05520.
[62] M. Aidelsburger, S. Nascimbene, and N. Goldman, Artificial gauge fields in materials and engineered systems, C.R. Phys. **19**, 394 (2018), quantum simulation/Simulation quantique.
[63] C. Hua Lee, Z. Papić, and R. Thomale, Geometric Construction of Quantum Hall Clustering Hamiltonians, Phys. Rev. X **5**, 041003 (2015).
[64] Z. Liu, A. Vaezi, C. Repellin, and N. Regnault, Phase diagram of $\nu = \frac{1}{2} + \frac{1}{2}$ bilayer bosons with interlayer couplings, Phys. Rev. B **93**, 085115 (2016).
[65] N. Read and E. Rezayi, Quasiholes and fermionic zero modes of paired fractional quantum hall states: The mechanism for non-Abelian statistics, Phys. Rev. B **54**, 16864 (1996).
[66] J. Dubail, N. Read, and E. H. Rezayi, Edge-state inner products and real-space entanglement spectrum of trial quantum hall states, Phys. Rev. B **86**, 245310 (2012).
[67] J. Dubail and N. Read, Entanglement Spectra of Complex Paired Superfluids, Phys. Rev. Lett. **107**, 157001 (2011).
[68] D. Vollhardt and P. Wölfle, *The Superfluid Phases Of Helium 3* (CRC Press, London, 1990).
[69] P. Di Francesco, P. Mathieu, and D. Sénéchal, *Conformal Field Theory* (Springer-Verlag, New York, 1997).
[70] J Voit, Charge-spin separation and the spectral properties of luttinger liquids, J. Phys. Condens. Matter **5**, 8305 (1993).
[71] T. Giamarchi, *Quantum Physics in One Dimension*, International Series of Monograph (Clarendon Press, Oxford, 2004).
[72] Y.-L. Wu, B. Estienne, N. Regnault, and B. A. Bernevig, Matrix product state representation of non-Abelian quasiholes, Phys. Rev. B **92**, 045109 (2015).
[73] M. P. Zaletel, R. S. K. Mong, and F. Pollmann, Topological Characterization of Fractional Quantum Hall Ground States from Microscopic Hamiltonians, Phys. Rev. Lett. **110**, 236801 (2013).
[74] M. P. Zaletel, R. S. K. Mong, F. Pollmann, and E. H. Rezayi, Infinite density matrix renormalization group for multicomponent quantum hall systems, Phys. Rev. B **91**, 045115 (2015).
[75] J. Haegeman, J. Ignacio Cirac, T. J. Osborne, and F. Verstraete, Calculus of continuous matrix product states, Phys. Rev. B **88**, 085118 (2013).
[76] M. Fannes, B. Nachtergaele, and R. F. Werner, Finitely correlated states on quantum spin chains, Commun. Math. Phys. **144**, 443 (1992).
[77] V. Crépel, B. Estienne, B. A. Bernevig, P. Lecheminant, and N. Regnault, Matrix product state description of halperin states, Phys. Rev. B **97**, 165136 (2018).
[78] C. Fernández-González, R. S. K. Mong, O. Landon-Cardinal, D. Pérez-García, and N. Schuch, Constructing topological models by symmetrization: A projected entangled pair states study, Phys. Rev. B **94**, 155106 (2016).
[79] M. Iqbal, K. Duivenvoorden, and N. Schuch, Study of anyon condensation and topological phase transitions from a $\mathbb{Z}_4$ topological phase using the projected entangled pair states approach, Phys. Rev. B **97**, 195124 (2018).
[80] F. A. Bais and J. K. Slingerland, Condensate-induced transitions between topologically ordered phases, Phys. Rev. B **79**, 045316 (2009).
[81] X. Chen, A. Roy, J. C. Y. Teo, and S. Ryu, From orbifolding conformal field theories to gauging topological phases, Phys. Rev. B **96**, 115447 (2017).
[82] A. Kitaev and J. Preskill, Topological Entanglement Entropy, Phys. Rev. Lett. **96**, 110404 (2006).
[83] M. Levin and X.-G. Wen, Detecting Topological Order in a Ground State Wave Function, Phys. Rev. Lett. **96**, 110405 (2006).
[84] J. Dubail, N. Read, and E. H. Rezayi, Real-space entanglement spectrum of quantum hall systems, Phys. Rev. B **85**, 115321 (2012).
[85] A. Sterdyniak, A. Chandran, N. Regnault, B. A. Bernevig, and P. Bonderson, Real-space entanglement spectrum of quantum hall states, Phys. Rev. B **85**, 125308 (2012).
[86] I. D. Rodríguez, S. H. Simon, and J. K. Slingerland, Evaluation of Ranks of Real Space and Particle Entanglement Spectra for Large Systems, Phys. Rev. Lett. **108**, 256806 (2012).
[87] V. Crépel, N. Claussen, B. Estienne, and N. Regnault, A variational approach to chiral topological order interfaces, Nat. Commun. **10**, 1861 (2019).
[88] V. Crépel, N. Claussen, N. Regnault, and B. Estienne, Microscopic study of the Halperin—Laughlin interface through matrix product states, Nat. Commun. **10**, 1860 (2019).
[89] T. H. Hansson, M. Hermanns, S. H. Simon, and S. F. Viefers, Quantum hall physics: Hierarchies and conformal field theory techniques, Rev. Mod. Phys. **89**, 025005 (2017).
[90] P. Ginsparg, Appl. Conformal Field Theory, arXiv:hep-th/9108028.